Three-Level Hybrid Active Power Filter with Quasi-Resonant DC-Link Technique in Three-Phase Four-Wire System

Bin Zhang, Io-Keong Lok, Ning-Yi Dai, Man-Chung Wong, Chi-Kong Wong
Department of Electrical and Computer Engineering
Faculty of Science and Technology, University of Macau
Macau S.A.R., P.R. China

***Abstract*—This paper presents a three-level hybrid active power filter (HAPF) combined with Quasi-Resonant DC-Link (QRDCL) soft-switching circuits in a three-phase four-wire system. Hybrid active power filter is a combined system of passive filter and active power filter, so it can compensate system harmonic current, reactive power and neutral current with a low dc voltage. Quasi-resonant dc-link circuits use the mirror symmetrical approach to achieve zero voltage switching for main switching devices in a three-level inverter in order to decrease switching power losses. By combining the hybrid active power filter and the soft-switching circuits, the proposed topology not only has a lower inverter rating but can also reduce switching power losses. Simulation results of this soft-switching hybrid active power filter are provided to verify this proposed system and its control strategy.**

I. INTRODUCTION

Nowadays, more nonlinear power devices are used in industrial field. Nonlinear loads cause harmonic currents, reactive power and excessive neutral current in three-phase four-wire system. Therefore, three-phase four-wire active power filter and hybrid active power filter are proposed to solve these power quality issues [1, 2].

Hybrid active power filter is a combined system of passive filter and active power filter. It can avoid parallel resonant between a source and a passive filter at some specific frequencies, moreover, hybrid active power filter reduces the power rating, initial costs and running costs of active power filter [3, 4]. So that, according to the different connections between passive filter and active filter, hybrid active power filters have several topologies and respective own characteristics [5]. In the recent years, hybrid active power filter has been developed in three-level structure, so that it can be used in high voltage applications [6].

Soft-switching techniques have been developed about several decades. Applying soft-switching techniques into power converters can reduce switching losses of power devices as well as release power stresses on devices, along with dv/dt and di/dt. As a result, the system efficiency is improved and life time of devices is prolonged. Quasi-resonant dc-link is an outstanding topology among soft-switching techniques. This circuit consists of a LC resonant circuit and two switches in dc side of the inverter, so it can build zero voltage switching for a two-level inverter. Two mirror symmetrical quasi-resonant dc-link circuits can be used in a three-level inverter [8]. Furthermore, soft-switching circuits have been applied in power compensators to reduce switching power losses and improve efficiency of compensation system [9, 10].

In this paper, quasi-resonant dc-link circuits are integrated into three-level hybrid active power filter in three-phase four-wire system as illustrated in Fig. 1. The passive filters of the hybrid active power filter are directly connected to the power system, and the active power filter is in series with the passive filter. Two quasi-resonant dc-link circuits are added to the dc bus of the inverter, as shown in the grey area. In section II, the operational principle and control of the quasi-resonant circuits are discussed. Section III provides the control system of the proposed hybrid active power filter combined with quasi-resonant dc-link circuits. Section IV presents the simulation results for verifying the validity of this proposed topology.

II. QUASI-RESONANT DC-LINK CIRCUITS IN THREE-LEVEL INVERTER

A. *Operational Principle of Quasi-Resonant DC-Link Circuit*

The controls of quasi-resonant dc-link circuits for three-level inverter have been reported in several papers [8, 10]. The upper equivalent circuit of quasi-resonant dc-link circuit in three-level inverter is illustrated in Fig. 2, and it is also marked in Fig. 1. The upper quasi-resonant bank includes two auxiliary

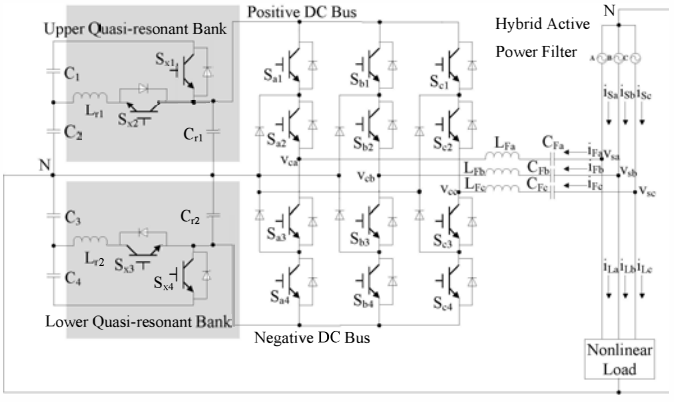

Fig. 1 Three-level hybrid active power filter combined with quasi-resonant dc-link circuits in three-phase four-wire system

switches S_{x1} and S_{x2}, a resonant inductor L_{r1}, a resonant capacitor C_{r1}, and the resonant period is T_{r1}. They form a second-order resonant circuit inside the inverter between two dc capacitors (C_1, C_2) and the inverter bridge. The dc capacitor C_1=C_2, so the voltage v_{c1}=v_{c2}, but the resonant capacitor C_{r1} is much smaller than C_1 or C_2. The current source I_{o1} indicates as an equivalent output current of the inverter, and the diode D_{inv1} represents the power diode which is anti-parallel with IGBT devices of the upper inverter, which are marked by dash line. The resonant waveform of this upper QRDCL circuit is shown in Fig. 3. The operation of this resonant circuit can be divided into five modes which are described as follow.

Mode A [before t_1]: before activating the resonant circuit, this is a normal state of the inverter. The auxiliary switch S_{x1} is conducted to clamp the input voltage limited to half of DC voltage, $V_{dc}/2$, so the resonant capacitor C_{r1} is charged up to the half of the normal dc voltage. The auxiliary switch S_{x2} is not conducted, so that the resonant is not activated. In addition, the voltages of the capacitor C_1 and C_2 are $V_{dc}/4$ respectively.

Mode B [t_1, t_2]: from Fig. 3 S_{inv1} represents switching state. When inverter switching state S_{inv1} should be changed at t_1, it needs to activate soft-switching first. After activating the resonant circuit at the time t_1, the clamping switch S_{x1} is turned off and the auxiliary switch S_{x2} is turned on. When the resonance begins, the voltage v_{r1} decreases rapidly, in the meantime the resonant current i_{r1} is increased rapidly, which are derived by the equations (1) and (2).

$$v_{r1} = \frac{V_{dc}}{4}[1+\cos(\omega_{r1}t)] \tag{1}$$

$$i_{r1}(t) = \frac{V_{dc}}{4Z_{r1}}\sin(\omega_{r1}t) \tag{2}$$

where the angular frequency of resonant circuit ω_{r1} is $1/\sqrt{L_{r1}C_{r1}}$, and the characteristic impedance $Z_{r1}=\sqrt{L_{r1}/C_{r1}}$. The energy stored in the capacitor C_{r1} is transferred to the capacitor C_2, which is passing the inductor L_{r1}.

Mode C [t_2, t_4]: this is a zero voltage or a near zero voltage interval, that is, in the vicinity of the first half resonant period $T_{r1}/2$. During this interval, the voltage v_{r1} of the capacitor C_{r1} is reduced to zero, that is, the dc-bus voltage of the inverter reaches zero. Moreover, the auxiliary switch S_{x2} is turned off at the time t_3, when the resonant current i_{r1} becomes zero even

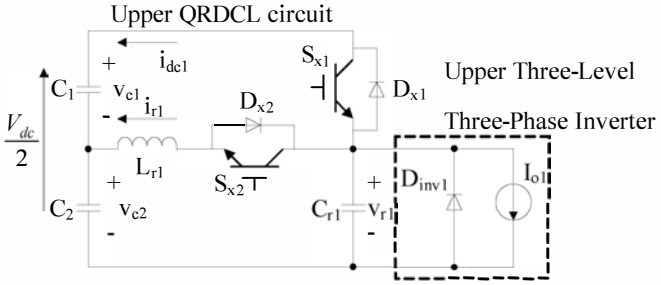

Fig. 2 Upper equivalent circuit of quasi-resonant dc-link circuit in three-level inverter

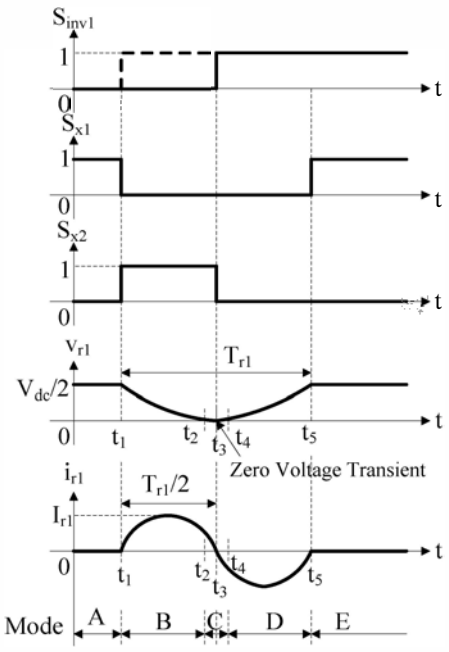

Fig. 3 Resonant waveforms and operational waveforms of the upper QRDCL inverter

reverse through anti-parallel diode D_{x2}, so the S_{x2} is obtained zero voltage and zero current turn off. Therefore, the switching state of the inverter is changed at this zero voltage switching period.

Mode D [t_4, t_5]: the resonant current i_{r1} is in the reverse direction flowing into the resonant capacitor C_{r1} during the second half resonant period from $T_{r1}/2$ to T_{r1}. The anti-parallel diode D_{x2} begins to conduct the resonant current, and the resonant energy is transferred back to the C_{r1} through the D_{x2}. Therefore, the C_{r1} is charged by this resonant current and the voltage v_{r1} of the C_{r1} increases rapidly.

Mode E [after t_5]: at the end of the resonant period T_{r1}, the voltage v_{r1} of the capacitor C_{r1} reaches the maximum value $V_{dc}/2$. The clamping switch S_{x1} is turned on under the nearly zero voltage, thus achieving zero voltage turn-on for the S_{x1}. The input voltage of the inverter is turned back to the dc voltage $V_{dc}/2$ and the inverter is connected to dc power capacitors C_1 and C_2 again. A resonant zero voltage switching cycle completes at this moment. The quasi-resonant circuit returns back to the normal steady-state as shown in Mode A, and it is also ready for the next soft-switching period.

B. Control Strategy of Quasi-Resonant DC-Link Circuit

If the switching state of the inverter is not changed, there is no soft-switching operation, so the quasi-resonant dc-link circuit will not be triggered. In this situation, the auxiliary switches S_{x1} and S_{x4} are in the on-state, meanwhile the auxiliary switches S_{x2} and S_{x3} are in the off-state. However, when a new switching pattern is detected by the ZVS detector, the quasi-resonant dc-link circuit is triggered. The waveforms of the resonant voltage and current of the QRDCL inverter are illustrated in Fig. 3. The dc voltage V_{dc} is assumed to be constant in one switching cycle. In the figure, the dash line of S_{inv1} represents the original PWM pattern of the inverter's

TABLE I SWITCHING TABLE OF UPPER QRDCL CIRCUITS

Mode	A	B	C		D	E
Time	before t_1	t_1~t_2	t_2~t_3	t_3~t_4	t_4~t_5	after t_5
Sx1	On	Off	Off	Off	Off	On
Sx2	Off	On	On	Off	Off	Off

main switches, while the solid lines of S_{inv1} represents the delayed PWM pattern due to QRDCL operation.

At the beginning of the soft-switching process, the PWM signals are being compared with the old PWM signals of the previous switching period. If the new PWM signals are detected, it triggers the corresponding QRDCL circuit immediately, that is, when the switching state of the inverter needs to be changed, old switching state will be held and the zero voltage switching controller will be triggered at t_1. Then, the auxiliary switch S_{x1} is turned off and the auxiliary switch S_{x2} is turned on. After waiting a delay time $T_{r1}/2$, when the zero voltage or near zero voltage condition appears, the new switching statue of the inverter will be active and latched. The auxiliary switches S_{x2} is turned off. In the end of the soft-commutation, the auxiliary switch S_{x1} is turned on. The switching function of an upper quasi-resonant dc-link circuit is summarized in Table I. The control of lower quasi-resonant bank is similar to the upper ones and can be derived.

III. CONTROL SYSTEM OF HYBRID ACTIVE POWER FILTER COMBINED WITH QUASI-RESONANT DC-LINK CIRCUITS

A. Design of Hybrid Active Power Filter

The hybrid active power filter consists of a three-phase passive filter and a three-level three-phase voltage source inverter. The resonant frequency of passive filter in each phase is given by equations (3).

$$f_F = \frac{1}{2\pi\sqrt{L_F C_F}} \tag{3}$$

where C_F is the coupling capacitor and L_F is the coupling inductance. The passive filter has a good filtering characteristic around the resonant frequency. The single phase reactive power of the passive filter Q_{CPF} can be defined in equation (4), where X_C and X_L are the coupling reactance. The required minimum dc-link voltage V_{dcmin} is expressed in equation (5) [2], where Q_L is the single phase reactive power of the load and V_S is the system voltage.

$$\frac{Q_{CPF}}{V_S^2} = \left(\frac{1}{X_C - X_L}\right) \tag{4}$$

$$V_{dc\min} = 2\sqrt{2}V_S\left|1 - \frac{Q_L}{|Q_{CPF}|}\right| \tag{5}$$

B. Control Sytem of Hybrid Active Power Filter combined with Quasi-Resonant DC-Link Circuits

The quasi-resonant dc-link circuits are added to hybrid active power filter in Fig. 1, so the overall control system of hybrid active power filter combined with quasi-resonant dc-link circuits is illustrated in Fig. 4. This system can be divided into three parts: calculate compensating current, pulse width modulation (PWM), and zero voltage switching control.

The compensating current is calculated by instantaneous reactive power theory [11], which has been widely applied in active power filter and hybrid active power filter. Three-phase system voltages (v_{Sa}, v_{Sb}, v_{Sc}) and currents (i_{Sa}, i_{Sb}, i_{Sc}) are measured and transformed into the αβ0 coordinate by transformations (6) and (7).

$$\begin{bmatrix} v_\alpha \\ v_\beta \\ v_0 \end{bmatrix} = \sqrt{2/3}\begin{bmatrix} 1 & -1/2 & -1/2 \\ 0 & \sqrt{3}/2 & -\sqrt{3}/2 \\ 1/\sqrt{2} & 1/\sqrt{2} & 1/\sqrt{2} \end{bmatrix}\begin{bmatrix} v_{Sa} \\ v_{Sb} \\ v_{Sc} \end{bmatrix} \tag{6}$$

$$\begin{bmatrix} i_\alpha \\ i_\beta \\ i_0 \end{bmatrix} = \sqrt{2/3}\begin{bmatrix} 1 & -1/2 & -1/2 \\ 0 & \sqrt{3}/2 & -\sqrt{3}/2 \\ 1/\sqrt{2} & 1/\sqrt{2} & 1/\sqrt{2} \end{bmatrix}\begin{bmatrix} i_{Sa} \\ i_{Sb} \\ i_{Sc} \end{bmatrix} \tag{7}$$

Real power $p_{\alpha\beta}$, reactive power $q_{\alpha\beta}$, and zero-phase sequence power p_0 are obtained in the αβ0 coordinate by (8). The ac part of real power $\tilde{p}_{\alpha\beta}$ is filtered by high pass filter (HPF).

$$\begin{bmatrix} p_{\alpha\beta} \\ q_{\alpha\beta} \\ p_0 \end{bmatrix} = \begin{bmatrix} v_\alpha & v_\beta & 0 \\ -v_\beta & v_\alpha & 0 \\ 0 & 0 & v_0 \end{bmatrix}\begin{bmatrix} i_\alpha \\ i_\beta \\ i_0 \end{bmatrix} \tag{8}$$

The compensating currents (i_{Sha}, i_{Shb}, i_{Shc}) are calculated by the inverse transform from $i_{C\alpha}$, $i_{C\beta}$, and i_{C0} in equation (9).

$$\begin{bmatrix} i_{C\alpha} \\ i_{C\beta} \\ i_{C0} \end{bmatrix} = \frac{1}{v_0 v_{\alpha\beta}^2}\begin{bmatrix} v_0 v_\alpha & -v_0 v_\beta & 0 \\ v_0 v_\beta & v_0 v_\alpha & 0 \\ 0 & 0 & v_{\alpha\beta}^2 \end{bmatrix}\begin{bmatrix} \tilde{p}_{\alpha\beta} \\ q_{\alpha\beta} \\ p_0 \end{bmatrix} \tag{9}$$

where $v_{\alpha\beta}^2 = v_\alpha^2 + v_\beta^2$.

Therefore, the reference voltages (v_{refa} , v_{refb} , v_{refc}) are derived by equation (10) [3, 4].

$$v_{refj} = K \cdot i_{Shj} \qquad \text{j=a, b, c} \tag{10}$$

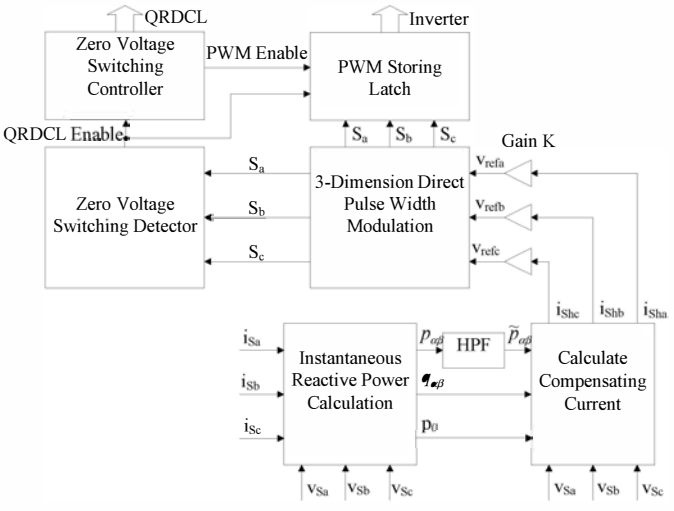

Fig. 4 Control system of hybrid active power filter combined with quasi-resonant dc-link circuits

The PWM control is implemented by the 3-dimension direct pulse width modulation, which is easy to implement and has low computation complexity among many other PWM algorithm [12]. The switching state and the pulse width of each phase are determined by the normalized three phase reference voltages in the following equation (11).

$$\vec{v}_{ref} = \vec{V}_{ref} / V_{dc} \tag{11}$$

The reference voltage vector is decomposed into two components: the offset voltage vector and the two-level voltage vector.

$$\vec{v}_{ref} = \vec{v}_{offset} + \vec{v}_{twol} \tag{12}$$

where $\vec{v}_{offset} = INT(\vec{v}_{ref})$, INT() means to remove the fractional part of the normalized voltage vector and get integer value.

Based on the volt-time product approximation, the pulse width of each phase can be calculated by (13)–(15). T_S is the sampling period, t_{offj} and t_{onj} are the dwell times of two adjacent output states. Therefore, the trigger signals of each power switches in three-level inverter are generated.

$$v_{refj} \cdot T_S = v_{offsetj} \cdot t_{offj} + (v_{offsetj} + 1) \cdot t_{onj} \quad j = a,b,c \tag{13}$$

$$t_{onj} = v_{twolj} \cdot T_S \quad j = a,b,c \tag{14}$$

$$t_{offj} = T_S - t_{onj} \quad j = a,b,c \tag{15}$$

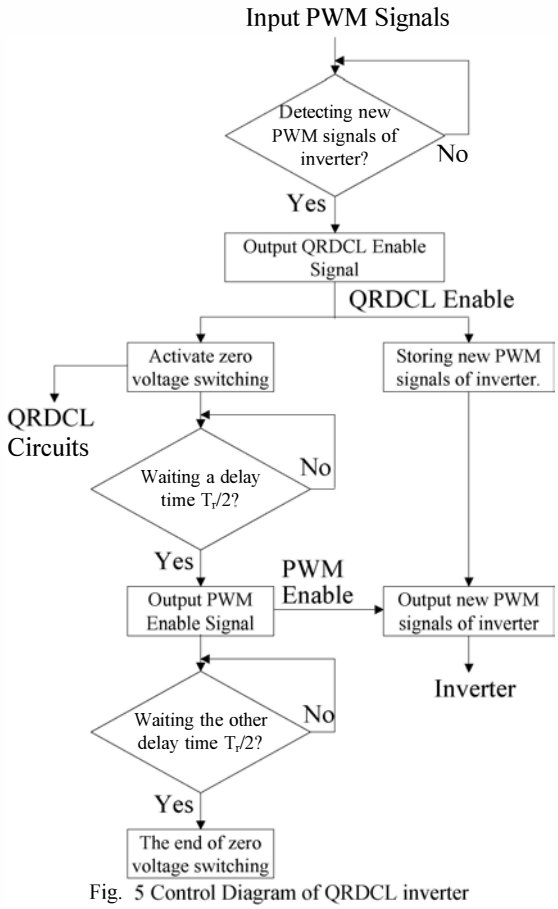

Fig. 5 Control Diagram of QRDCL inverter

The detail control strategy and operating principle of QRDCL circuit are described in Section II. To cooperate PWM and soft-switching, the control diagram of QRDCL inverter is illustrated in Fig. 5. In order to achieve the soft-switching, the PWM signals are sent to the PWM Storing Latch instead of directly sending to the power switches. When the Zero Voltage Switching Detector detects new PWM signals, it sends the QRDCL Enable signal to activate the zero voltage switching operation and store new PWM signals, then the storing latch waits for the PWM Enable signal. Once the QRDCL circuit is triggered, and the resonant begins, the zero voltage switching controller waits a delay time for the zero voltage condition. When the zero voltage condition appears, the PWM Enable signal will be sent to PWM Storing Latch and the new PWM signal will be outputted to the inverter, so that zero voltage switching for the inverter is achieved. In the second half of the resonant period T_r, it also waits a delay time $T_r/2$ to get the end of the zero voltage switching, then QRDCL inverter goes to normal state and waits next soft-commutation.

IV. Simulation Results

The hybrid active power filter with a mirror symmetrical pair of quasi-resonant dc-link circuits in three-phase four-wire system is illustrated in Fig. 1. This simulation software is PSCAD /EMTDC. The system voltages are balanced, but the system loads are nonlinear loads which produce harmonic currents. The system parameters are summarized in Table II. The passive filter is selected the third-order filter circuit, and the gain K is 50 to achieve a broad filtering frequency field.

Three-phase system currents (i_{sa}, i_{sb}, i_{sc}) and neutral current (i_{sn}) before compensation is shown in Fig. 6, which is not sinusoidal waveform including harmonic currents and reactive power required to eliminate. Fig. 7 and Fig. 8 show the system current after compensation in hard-switching and soft-

TABLE II HAPF Combined with QRDCL Circuits in Three-Phase Four-Wire System

System Parameters	Symbols	Value
Source Voltage (RMS)	V_S	220V
Source Frequency	F_S	50Hz
System Inductance	L_S	1mH
Coupling Capacitance	C_F	66μF
Coupling Inductance	L_F	17mH
Switching Frequency	f_{SW}	5kHz
DC Voltage	V_{dc}	100V
DC Capacitors	C_1, C_2, C_3, C_4	5000μF
Resonant Inductors	L_{r1}, L_{r2}	2.533μH
Resonant Capacitors	C_{r1}, C_{r2}	1μF

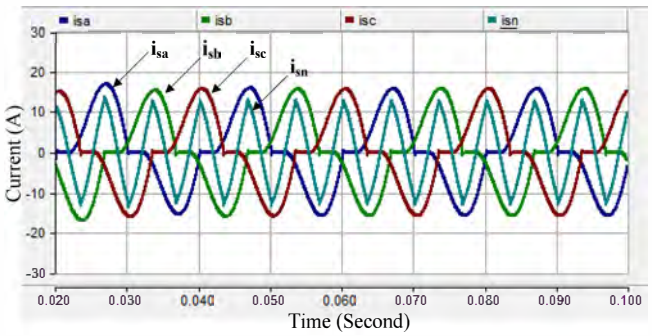

Fig. 6 Three-phase system currents and neutral current before compensation

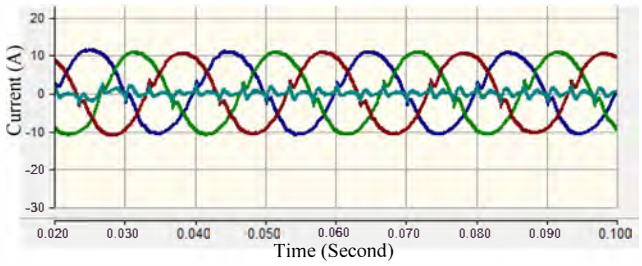

Fig. 7 Three-phase system currents and neutral current after compensation in hard-switching

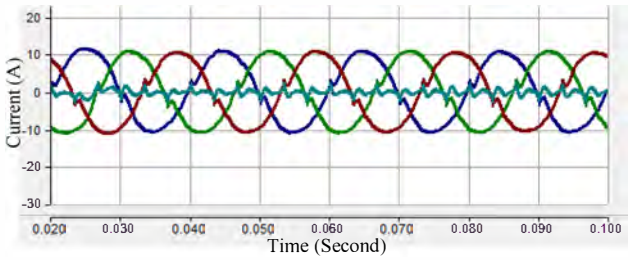

Fig. 8 Three-phase system currents and neutral current after compensation in soft-switching

switching respectively. From these compensating results, they show that this proposed topology can compensate well in both hard-switching and soft-switching. Since the quasi-resonant dc-link operation affects the compensation performance of the power compensator, the compensation result is slight different from the hard-switching one. The detail results are listed in Table III. The total switching loss in hard-switching is illustrated in Fig.9 (a), however, the total switching loss in soft-switching is shown in Fig. 10 (a). By comparing both simulation results, it is proved that quasi-resonant dc-link circuits can significantly reduce the switching losses of power device. Fig. 9 (b) and Fig. 10 (b) are also shown the signficant reduction of switching losses in detail. The soft-switching function indeed reduces switching losses and improve the system efficiency. The average switching loss of the proposed system is from 3.35W in hard-switching to 2.51W in soft-switching. The average switching loss have been reduced about 25%. Moreover, the measured rating of the soft-switching inverter of the propose topology is 1kW.

Fig. 11 shows the switching transition of power device in hard-switching and soft-switching. The voltage v_{ce} and current i_{ce}, which is multiplied five to show, of power device are clearly shown that the switching stress is reduced and the change rate of the voltage is released with zero voltage switching. Moreover, the life time of the power devices can be prolonged.

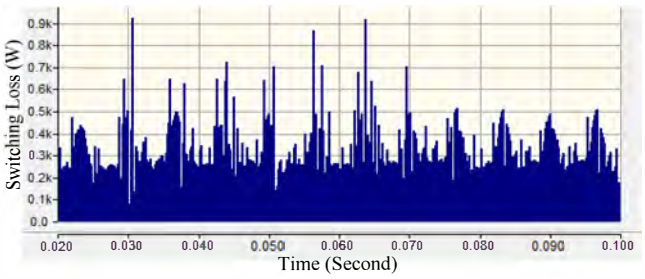

(a)

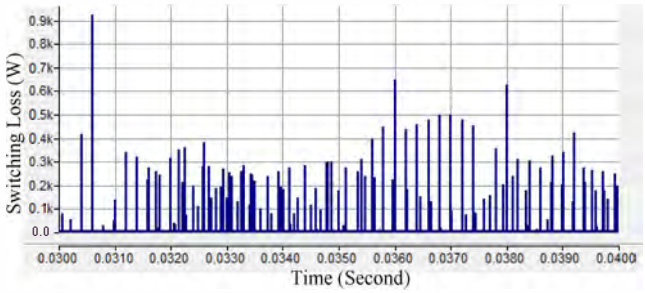

(b)

Fig. 9 Switching loss in hard-switching:
(a) total switching loss; (b) switching losses within 0.01s.

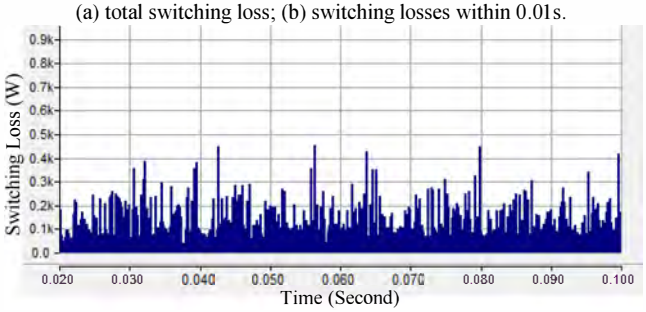

(a)

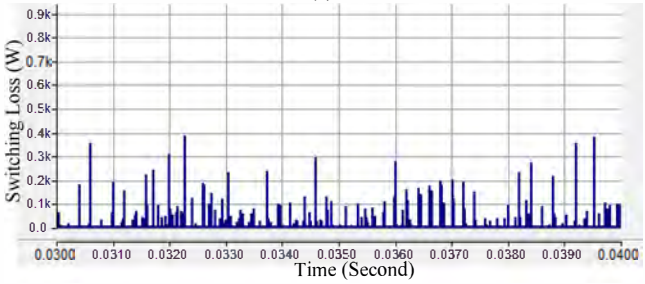

(b)

Fig. 10 Switching loss in soft-switching:
(a) total switching loss; (b) switching losses within 0.01s.

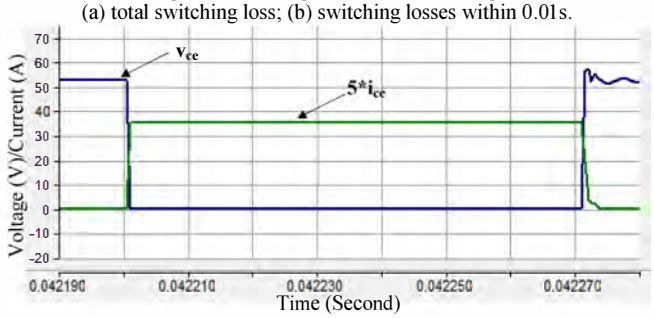

(a)

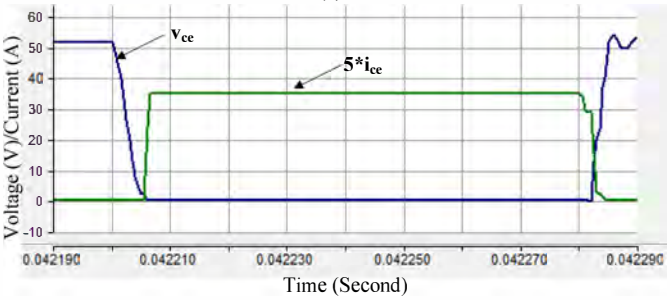

(b)

Fig. 11 Switching transition of power device:
(a) hard-switching; (b) soft-switching.

TABLE III SIMULATION RESULTS OF HYBRID ACTIVE POWER FILTER COMBINED WITH QUASI-RESONANT DC-LINK CIRCUITS

		Before Compensation	After Compensation	
			Hard-Switching	Soft-Switching
THD	Phase A	30.2%	6.99%	7.26%
	Phase B	30.2%	7.36%	7.61%
	Phase C	30.2%	7.02%	7.28%
Power Factor	Phase A	0.84	1.00	1.00
	Phase B	0.84	1.00	1.00
	Phase C	0.84	1.00	1.00
Neutral Current (RMS)		7.62A	0.76A	0.77A
Average Switching Losses		---	3.35W	2.51W

V. CONCLUSION

In this paper, QRDCL soft-switching technique is applied to hybrid active power filter in a three-phase four-wire system. The soft-switching circuits can reduce switching losses and improve efficiency of the hybrid active power filter. The control system of the hybrid active power filter is implemented to achieve harmonic current, reactive power and neutral current compensation. The proposed three-level hybrid active power filter combined with quasi-resonant dc-link circuits is validated by the simulation results. Results indicate that harmonic current, reactive current and neutral currents are compensated simultaneously. In addition, the switching losses can be reduced up to 25% after soft-switching is applied.

ACKNOWLEDGMENT

This work was supported by the Science and Technology Development Fund (FDCT) of Macau S.A.R., with project code: 007-2007-A1, and the Research Committee of University of Macau.

REFERENCES

[1] Ning-Yi Dai, Man-Chung Wong, and Ying-Duo Han, "Application of a three-level NPC inverter as a three-phase four-wire power quality compensator by generalized 3DSVM," IEEE Trans. on Power Electronics, Vol. 21, No. 2, March 2006, pp. 440–449.

[2] Chi-Seng Lam, Wai-Hei Choi, Man-Chung Wong, and Ying-Duo Han, "Adaptive dc-link voltage-controlled hybrid active power filters for reactive power compensation," IEEE Trans. on Power Electronics, Vol. 27, No. 4, April, 2012, pp. 1758–1772.

[3] F. Z. Peng, H. Akagi, and A. Nabae, "A new approach to harmonic compensation in power systems," Industry Application Society Annual Meeting, 1988, pp. 874–880.

[4] Hideaki Fujita, and Hirofumi Akagi, "A practical approach to harmonic compensation in power systems–series connection of passive and active filters," IEEE Trans. on Industry Applications, Vol. 27 No. 6, November/December, 1991, pp. 1020–1025.

[5] Man-Chung Wong, Chi-Seng Lam, and Ning-Yi Dai, "Comparison of structure topologies for hybrid filters," Universities Power Engineering Conference, 2008, pp. 1–5.

[6] Hirofumi Akagi, and Takaaki Hatada, "Voltage balancing control for a three-level diode-clamped converter in a medium-voltage transformerless hybrid active filter," IEEE Trans. on Power Electronics, Vol. 24, No. 3, March, 2009, pp. 571–579.

[7] Maria D. Bellar, Tzong-Shiann Wu, Aristide Tchamdjou, Javad Mahdavi, and M. Ehsani, "A review of soft-switched dc-ac converters," IEEE Trans. on Industry Applications, Vol. 34, No. 4, July/August, 1998, pp. 847–860.

[8] Jie Chang, and Jun Hu, "Modular design of soft-switching circuits for two-level and three-level inverters," IEEE Trans. on Power Electronics, Vol. 21, No. 1, January, 2006, pp. 131–139.

[9] Ming-Hui Zhan, Man-Chung Wong, and Ying-Duo Han, "Quasi-resonant dc link control of 3-dimensional hysteresis current pwm technique in 3-phase 4-wired power quality compensator," Transmission and Distribution Conference and Exhibition: Asia and Pacific, 2005, pp. 1–6.

[10] Io-Keong Lok, and Man-Chung Wong, "Quasi-resonant dc-link control of three-level active power filter," Universities Power Engineering Conference, 2008, pp. 1–5.

[11] Hirofumi Akagi, Yoshihira Kanazawa, and Akira Nabae, "Instantaneous reactive power compensators comprising switching devices without energy storage components," IEEE Trans. on Industry Application, Vol. IA-20, No.3, May/June, 1984, pp. 625–630.

[12] Ning-Yi Dai, Man-Chung Wong, Yuan-Hua Chen, and Ying-Duo Han, "A 3-D generalized direct pwm algorithm for multilevel converters," IEEE Power Electronics Letters, Vol. 3, No. 3, September, 2005, pp. 85–88.

[13] Io-Keong Lok, Ning-Yi Dai, and Man-Chung Wong, "A three-level soft-switching active power filter with dc self-balancing capability," International Review of Electrical Engineering (I. R. E. E.), Vol. 6, No. 7, November-December, 2011, pp. 2883–2893.

[14] Chi-Seng Lam and Man-Chung Wong, "System and control design of a hybrid active power filter in three-phase four-wire system," Power Electronics System and Applications, 2009, PESA 2009, 3rd International Conference, pp. 1-5.

[15] Chi-Seng Lam, Xiao-Xi Cui, Man-Chung Wong, and Ying-Duo Han, "Minimum dc-link voltage design of three-phase four-wire active power filter," Control and Modeling for Power Electronics 2012, pp. 1-5.